

# Interaction of the spike protein RBD from SARS-CoV-2 with ACE2: similarity with SARS-CoV, hot-spot analysis and effect of the receptor polymorphism

Houcemeddine Othman<sup>1\*</sup>, Zied Bouzlama<sup>2</sup>, Jean-Tristan Brandenburg<sup>1</sup>, Jorge da Rocha<sup>1</sup>, Yosr Hamdi<sup>3</sup>, Kais Ghedira<sup>4</sup>, Najet Srairi-Abid<sup>5</sup>, Scott Hazelhurst<sup>1,6</sup>

<sup>1</sup> Sydney Brenner Institute for Molecular Bioscience, Faculty of Health Sciences, University of the Witwatersrand, Johannesburg, South Africa.

<sup>2</sup> Laboratory of veterinary epidemiology and microbiology LR16IPT03. Institut Pasteur of Tunis. University of Tunis El Manar, Tunis, Tunisia.

<sup>3</sup> Laboratory of Biomedical Genomics and Oncogenetics, LR16IPT05, Pasteur Institute of Tunis, University of Tunis El Manar, Tunis, Tunisia.

<sup>4</sup> Laboratory of Bioinformatics, Biomathematics and Biostatistics - LR16IPT09, Pasteur Institute of Tunis, University of Tunis El Manar, Tunis, Tunisia.

<sup>5</sup> Université de Tunis El Manar, Institut Pasteur de Tunis, LR11IPT08 Venins et Biomolécules Thérapeutiques, 1002, Tunis, Tunisia.

<sup>6</sup> School of Electrical and Information Engineering, University of the Witwatersrand, Johannesburg, South Africa.

\* [houcemoo@gmail.com](mailto:houcemoo@gmail.com), [houcemeddine.othman@wits.ac.za](mailto:houcemeddine.othman@wits.ac.za)

## Abstract

The spread of COVID-19 caused by the SARS-CoV-2 outbreak has been growing since its first identification in December 2019. The publishing of the first SARS-CoV-2 genome made a valuable source of data to study the details about its phylogeny, evolution, and interaction with the host. Protein-protein binding assays have confirmed that Angiotensin-converting enzyme 2 (ACE2) is more likely to be the cell receptor through which the virus invades the host cell. In the present work, we provide an insight into the interaction of the viral spike Receptor Binding Domain (RBD) from different coronavirus isolates with host ACE2 protein. By calculating the

binding energy score between RBD and ACE2, we highlighted the putative jump in the affinity from a progenitor form of SARS-CoV-2 to the current virus responsible for COVID-19 outbreak. Our result was consistent with previously reported phylogenetic analysis and corroborates the opinion that the interface segment of the spike protein RBD might be acquired by SARS-CoV-2 via a complex evolutionary process rather than a progressive accumulation of mutations. We also highlighted the relevance of Q493 and P499 amino acid residues of SARS-CoV-2 RBD for binding to human ACE2 and maintaining the stability of the interface. Moreover, we show from the structural analysis that it is unlikely for the interface residues to be the result of genetic engineering. Finally, we studied the impact of eight different variants located at the interaction surface of ACE2, on the complex formation with SARS-CoV-2 RBD. We found that none of them is likely to disrupt the interaction with the viral RBD of SARS-CoV-2.

key words: COVID-19, ACE2, viral spike Receptor Binding Domain, homology-based protein-protein docking, variants.

## 1 Introduction

The coronavirus SARS-CoV-2 (previously known as nCoV-19) has been associated with the recent epidemic of acute respiratory distress syndrome [2]. Recent studies have suggested that the virus binds to the ACE2 receptor on the surface of the host cell using spike proteins, and explored the binary interaction of these two partners [8, 23]. In this work, we focused our analysis on the interface residues to get insight into four main subjects: (1) The architecture of the spike protein interface and whether its evolution in many isolates supports an increase in affinity toward the ACE2 receptor; (2) How the affinity of SARS-COV-2-RBD and SARS-CoV-RBD toward different ACE2 homologous proteins from different species is dictated by a divergent interface sequences (3); A comparison of the interaction hotspots between SARS-CoV and SARS-CoV-2; and finally, (4) whether any of the studied ACE2 variants may show a different binding property compared to the reference allele. To tackle these questions we used multi-scale modelling approaches in combination with sequence and phylogenetic analysis.

## 2 Materials and Methods

### 2.1 Sequences and data retrieval

Full genome sequences of 10 Coronaviruses isolates were retrieved from NCBI Genbank corresponding to the following accession numbers: AY485277.1 (SARS coronavirus Sino1-11), FJ882957.1 (SARS coronavirus MA15), MG772933.1 (Bat SARS-like coronavirus isolate bat-SL-CoVZC45), MG772934.1 (Bat SARS-like coronavirus isolate bat-SL-CoVZXC21), DQ412043.1 (Bat SARS coronavirus Rm1), AY304488.1 (SARS coronavirus SZ16), AY395003.1 (SARS coronavirus ZS-C), KT444582.1 (SARS-like coronavirus WIV16), MN996532.1 (Bat coronavirus RaTG13) in addition to Wuhan seafood market pneumonia virus commonly known as SARS-CoV-2 (accession MN908947.3).

The sequences of the surface glycoprotein were extracted from the Coding Segment (CDS) translation feature from each genome annotation or by locally aligning the protein from SARS-CoV-2 with all possible ORFs from the translated genomes. ACE2 orthologous sequences from Human (Uniprot sequence Q9BYF1), Masked palm civet (NCBI protein AAX63775.1 from *Paguma larvata*), Chinese rufous horseshoe bat (NCBI protein AGZ48803.1 from *Rhinolophus sinicus*), King cobra snake (NCBI protein ETE61880.1 from *Ophiophagus hannah*), chicken (NCBI protein XP\_416822.2, *Gallus gallus*), domestic dog (NCBI protein XP\_005641049.1, *Canis lupus familiaris*), pig (NCBI protein XP\_020935033.1, *Sus scrofa*) and Brown rat (NCBI protein NP\_001012006.1 *Rattus norvegicus*) were also computed and retrieved.

Human variants of the ACE2 gene were collected from the gnomAD database. Only variants that map to the protein coding region and belonging to the interface of interaction with the RBD of the spike protein were retained for further analyses.

### 2.2 Sequence analysis and phylogenetic tree calculation

MAFFT 7.450 was used to align the whole genome sequences and the protein sequences of viral RBDs [5] (Supplementary Materials 1). Prediction of

the N-Glycosylation sites was made for all studied ACE2 sequences using 51  
NetNGlyc server (<https://www.cbs.dtu.dk/services/NetNGlyc/>). For 52  
the genome comparison, we selected the best site model based on lowest 53  
Bayesian Information Criterion (BIC) calculated using model selection 54  
tool implemented in MEGA 6 software [16]. The General Time Reversible 55  
(GTR) model was chosen as the best fitting model for nucleotide substitution 56  
with discrete Gamma distribution (+G) with 5 rate categories. For the 57  
RBD sequences, the best substitution model for maximum likelihood (ML) 58  
calculation was selected using a model selection tool implemented on MEGA 59  
6 software based on the lowest BIC score. Therefore, the WAG model [20] 60  
using a discrete Gamma distribution (+G) with 5 rate categories has been 61  
selected. 62

Phylogenetic trees were generated using a ML method in MEGA 6. The 63  
consistency of the topology, for the RBD sequences, was assessed using a 64  
bootstrap method with 1000 replicates. The resulting phylogenetic tree 65  
was edited with iTOL [9]. 66

### 2.3 Homology based protein-protein docking and binding 67 energy scores estimation 68

The co-crystal structure of the spike protein of SARS-CoV complexed 69  
to human-civet chimeric receptor ACE2 was solved at 3 Å of resolution 70  
(PDB code 3SCL). We used this structure as a template to build the 71  
complex of spike protein from different virus isolates with the human ACE2 72  
protein (Uniprot sequence Q9BYF1). The template sequences of the ligand 73  
(spike protein) and the receptor (ACE2) were aligned locally with the 74  
target sequences using the program Water from the EMBOSS package [12]. 75  
Modeller version 9.22 [14] was then used to predict the complex model of 76  
each spike protein with the ACE2 using a slow refining protocol. For each 77  
model, we generated ten conformers from which we selected the model with 78  
the best DOPE score [15]. 79

To calculate the binding energy scores we used, PRODIGY server [22], 80  
MM-GBSA method implemented in the HawkDock server [19] and FoldX5 81  
[3]. The contribution of each amino acid in protein partners was calculated 82  
HawkDock server. Different 3D structures of human ACE2 (hACE2), 83



each comprising one of the identified variants, were modeled using the BuildModel module of FoldX5. Because it is more adapted to predict the effect of punctual variations of amino acids, we used DynaMut at this stage of analysis [13].

## 2.4 Flexibility analysis

We ran a protocol to simulate the spike RBD fluctuation of SARS-CoV-2 and SARS-CoV using the standalone program CABS-flex (version 0.9.14) [7]. Three replicates of the simulation with different seeds were conducted using a temperature value of 1.4 (dimensionless value related to the physical temperature). The protein backbone was kept fully flexible and the number of the Monte Carlo cycles was set to 100.

## 3 Results

### Sequence and phylogenetic analysis

Phylogenetic analysis of the different RBD sequences revealed two well supported clades. Clade 1 includes Rm1 isolate, Bat-SL-CoVZC45 and Bat-SL-CoVZXC21. These three isolates are closely related to SARS-CoV-2 as revealed by the phylogenetic tree constructed from the entire genome (Figure 1A). Clade 2 includes SARS-CoV-2, RatG13, SZ16, ZS-C, WIV16, MA15, and SARS-CoV-Sino1-11 isolates (Figure 1A). SARS-CoV-2 and RatG13 sequences are the closest to the common ancestor of this clade. The exact tree topology is reproduced when we used only the RBD segment corresponding to the interface residues with hACE2. This is a linear sequence spanning from residue N481 to N501 in SARS-CoV-2.

Multiple sequence alignment showed that the interface segment of SARS-CoV-2 shares higher similarity to sequences from clade 2 (Figure 1B). However, we noticed that S494, Q498 and P499 are exclusively similar to their equivalent amino acids in sequences from clade 1. SARS-CoV-2 interface sequence is closely related to RaTG13 sequence, isolated from *Rhinolophus affinis* bat.

6

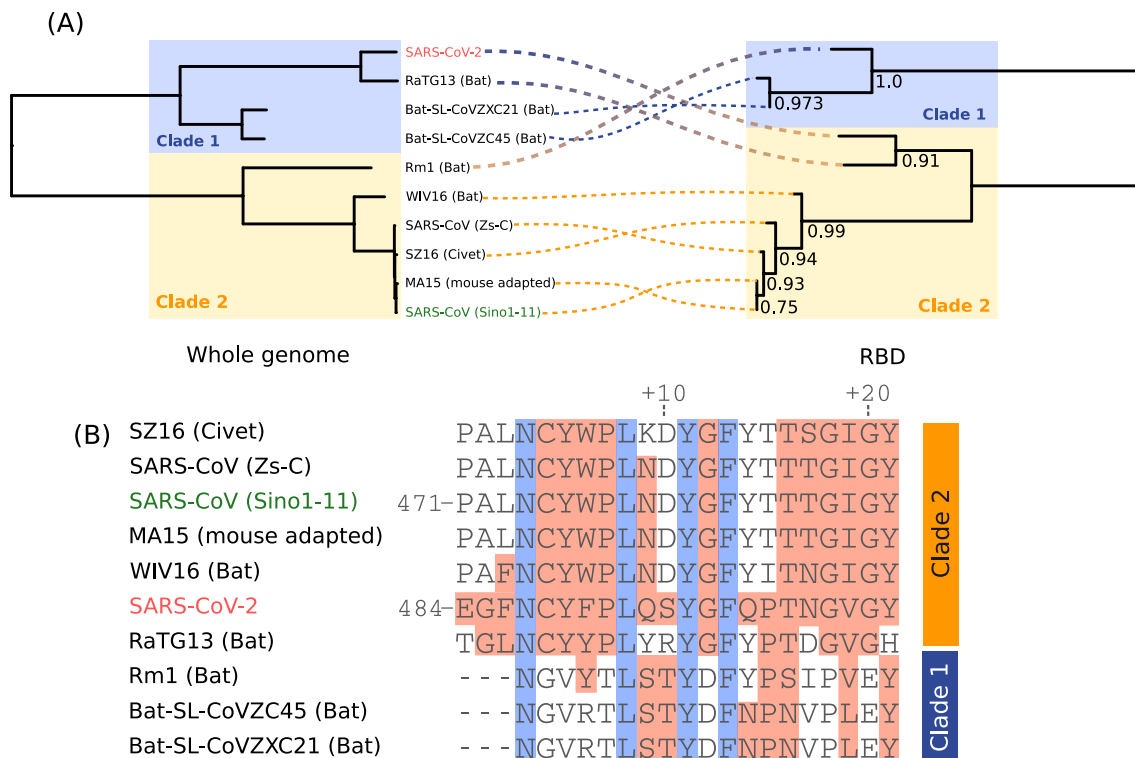


**Figure 1.** Phylogenetic and sequence analysis based on full genomes and RBDs from the different isolates included in this study. (A) Phylogeny trees are opposed to each other to show the clade discrepancies and discontinuous lines shows the equivalent taxon between each tree. (B) Multiple sequence alignment of the interface residues of RBD. Blocks in red color indicate the residues with similar biochemical properties to the positions in SARS-CoV-2. Conserved residues are colored in blue.

### 3.1 Prediction of the RBD/hACE2 complex structure

To investigate whether the interface of the spike protein isolate evolves by increasing the affinity toward the ACE2 receptor in the final host, we predicted the interaction models of the envelope anchored spike protein (SP) from several clinically relevant coronavirus isolates with hACE2 receptor (PDB files for the complexes are listed in Supplementary Materials 1). The construction of the complex applies a comparative-based approach that uses a template structure in which both partners (ligand and receptor) are closely related to those in the target system respectively. In our study, we only modeled the interaction of the RBD which was shown to be implicated in the

physical interaction with ACE2 (Figure 2A). The lowest sequence identity of the modeled spike proteins as well as those of any of the orthologous ACE2 sequences (Human, civet, bat, pig, rat, chicken and snake) do not fall below 63% toward their respective templates. At such values of sequence identities it is expected that the template and the target complexes share the same binding mode [6].

### **3.2 Analysis of the interaction energy scores of hACE2 with other virus isolates**

We calculated the binding energy scores of the RBD from different virus isolates interacting with hACE2 (Figure 2b). All three methods used for the calculation are in agreement that RBDs from bat-SL-CoVZC45, bat-SL-CoVZXC21 and Rm1 show the worst energy scores. While the binding energy score falls in the boundary limit of the uncertainty margin for PRODIGY calculation (section 2, Supplementary material 2), the differences in the scores calculated by FoldX and MM-GBSA are not. Therefore we consider that such differences in energies compared to SARS-CoV-2 are consistent between the three methods. Except for FoldX, the affinity is predicted to be more favorable for RBD from SARS-CoV-2 compared to SARS-CoV. However, MM-GBSA only marginally discriminates between the two values.

### **3.3 Interaction of RBD from SARS-CoV-2 and SARS-CoV with different ACE2 orthologues**

To investigate the tendency of SARS-CoV-2 and SARS-CoV to interact with different orthologous forms of ACE2, we analysed the divergence in their respective interacting surfaces. We have also mapped the putative glycosylation sites that overlap with the interface with RBD. Overall, the binding energy scores are similar between SARS-CoV-2 and SARS-CoV considering the estimation of error for each method. Variances are more important for the calculations made by FoldX and although of different formalism, MM-GBSA and PRODIGY scores are relatively in agreement. Compared to hACE2, only the Canidae form shows better energy scores

8

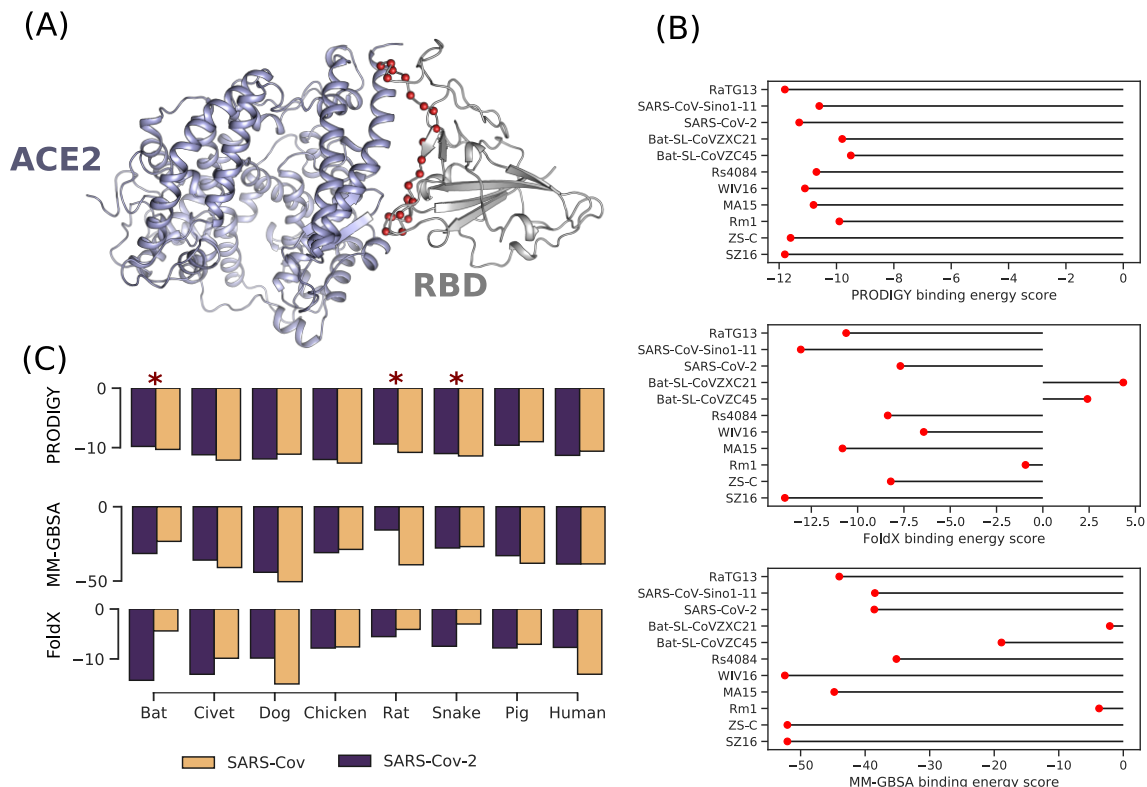


**Figure 2.** Homology based protein-protein docking of RBD/ACE2 and binding energy score analysis of spike RBD with ACE2 receptor. (A) Homology based protein-protein docking complex of SARS-CoV-2 RBD with hACE2. The red spheres are the interface residues of the RBD. (B) Binding energy scores calculated with PRODIGY, MM-GBSA and FoldX methods for RBDs from different coronaviruses forms with hACE2. (C) Binding energy scores of RBDs from SARS-CoV-2 and SARS-CoV interacting with ACE2 orthologues. Asterisks indicate the putative overlap of a glycosylation site with the protein-protein interface

both in PRODIGY and MM-GBSA for SARS-CoV-2. Moreover, We found 155  
that putative glycosylation sites overlap significantly with RBD interaction 156  
in Snake, Rat and Bat forms (section 3, Supplementary data 2).The docking 157  
also shows that key residues of RBD SARS-CoV-2 tend to interact with 158  
conserved residues on ACE2 (Figure 3, Supplementary data 2) (residues 159  
36-53 in hACE2) which can explain the similar values of energy scores. 160

### 3.4 Decomposition of the interaction energy 161

MM-GBSA allowed us to assign the contribution of each amino acid in 162  
the interface with hACE2, in the binding energy score. We conducted this 163  
analysis using both sequences of the SARS-CoV-2 Wuhan-Hu-1 (Figure 3A) 164  
and the Sino1-11 SARS-CoV (Figure 3B) isolates. Residues F486, Y489, 165  
Q493, G496, T500 and N501 of SARS-CoV-2 RBD forming the hotspots of 166  
the interface with hACE2 protein were investigated (we only consider values 167  
> 1 or < 1 kcal/mol to ignore the effect due to the thermal fluctuation). 168  
All these amino acids form three patches of interaction spread along the 169  
linear interface segment (Figure 3C): two from the N and C termini and one 170  
central. T500 establishes two hydrogen bonds using its side and main chains 171  
with Y41 and N330 of hACE2. N501 forms another hydrogen bond with 172  
ACE2 residue K353 buried within the interface. On the other hand, SARS- 173  
CoV RBD interface contains five residues (Figure 3D), L473, Y476, Y485, 174  
T487 and T488 corresponding to the equivalent hotspot residues of RBD 175  
from SARS-CoV-2 F487, Y490, G497, T501 and N502. Therefore, Q493 as 176  
a hotspot amino acid is specific to SARS-CoV-2 interface. The equivalent 177  
residue N480 in SARS-CoV only shows a non-significant contribution of 178  
0.18 kcal/mol. 179

The similarity matrix analysis was conducted to assess the divergence of 180  
the interaction interface of RBDs qualitatively, i.e. the specific set of residues 181  
implicated in the interaction with ACE2, and quantity, i.e. the contribution 182  
of each residue in the binding energy score. The similarity matrix was 183  
calculated from free energy decomposition of interface residues of RBDs 184  
from SARS-CoV-2 and SARS-CoV in complex with ACE2 orthologous 185  
and reported as a network representation (Figure 3E and Figure 1 and 186  
2 in Supplementary Materials 2). We noticed the existence of densely 187  
interconnected edges involving all the protein-protein complexes for SARS- 188  
CoV-2 and SARS-CoV except those involving ACE2 from *Sus scrofa* and 189  
*Rattus norvegicus*. Complexes involving the RBD of SARS-CoV-2 show less 190  
intrinsic similarity compared to RBD of SARS-CoV. However, similarity 191  
scores tend to be uniform in the group involving ACE2 from human, civet, 192  
dog, bat, snake, and chicken. The complex including hACE2 does not seem 193  
to diverge from the rest of the members of the SARS-CoV-2 group such as 194  
the case of *Sus scrofa* and *Rattus norvegicus*. 195

### 3.5 Flexibility analysis

196

Sequence analysis and the visual inspection of RBD/hACE2 complex might 197  
reflect the substitution of P499 in SARS-CoV-2 RBD as a form of adaptation 198  
toward a better affinity with the receptor. In order to further investigate 199  
its role, we performed a flexibility analysis using a reference structure 200  
(SARS-CoV-2 RBD containing P499) and an *in silico* mutated form P499T, 201  
a residue found in SARS-CoV and most of the clade 2. Our results show 202  
that the mutation caused a significant decrease in stability for nine residues 203  
of the interface corresponding to segment 482-491 (Figure 3F). Indeed, the 204  
RMSF variability per amino acid for this sequence increases compared to 205  
the reference structure. 206

### 3.6 Analysis of ACE2 variability and affinity with the virus

207

208

A total of eight variants of hACE2 that map to the interaction surface 209  
are described in the gnomAD database (Figure 4A). All these variants are 210  
rare (Table 1) and mostly found in European non-Finnish and African 211  
populations. Considering both the enthalpy ( $ddG$ ) and the vibrational 212  
entropy in our calculation ( $dds$ ), we found no significant changes ( $> 1$  or 213  
 $< 1$  kcal/mol) in neither the folding energy of the complex (Figure 4B) nor 214  
the interaction energy of the protein-protein partners (Figure 4C). 215

## 4 Discussion

216

Since the Covid-2019 outbreak, several milestone papers have been published 217  
to examine the particularity of SARS-CoV-2 spike protein and its putative 218  
interaction with ACE2 as a receptor [21]. In the current study, we focused 219  
our analysis on the interface segments of SARS-CoV-2 spike RBD interacting 220  
with ACE2 from different species by estimating interaction energy profiles. 221

We have studied the effect of eight variants of ACE2 in order to detect 222  
polymorphisms that may increase or decrease virulence in the host. Our 223  
results showed that if ACE2 is the only route for the infection in humans, 224  
variants interacting physically with RBD are not likely to disrupt the 225  
formation of the complex and would have a marginal effect on the affinity. 226

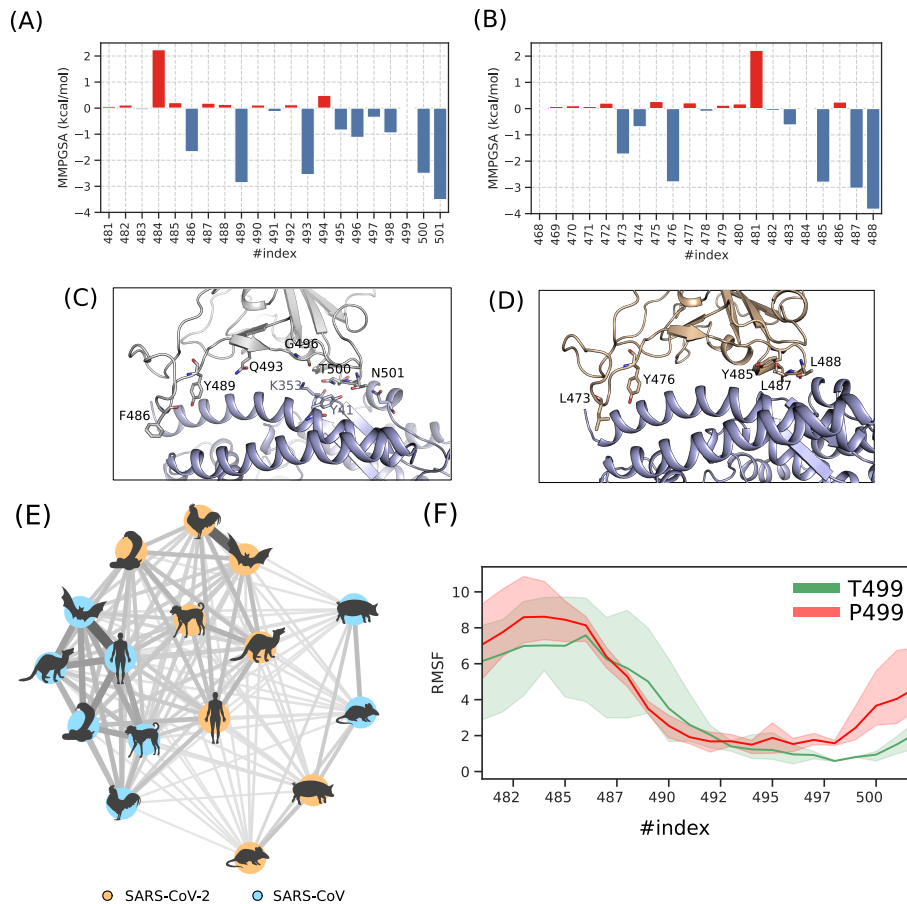


**Figure 3.** Analysis of the interaction between RBD and hACE2. Decomposition of the MM-GBSA energy for each amino acid of the binding surface from SARS-CoV-2 (A) and SARS-CoV Sino1-11 isolate (B). Position of the hotspot residues of the complexes RBD-SARS-CoV-2/hACE2 (C) and RBD-SARS-CoV/hACE2 (D). (E) similarity matrix in network representation calculated from the free energy decomposition profiles of complexes involving SARS-CoV-2 and SARS-CoV RBDs interacting with different orthologous sequences of ACE2. (F) Flexibility of RBD interface residue expressed as Root Mean Square Fluctuation (RMSF) for two forms of RBD-SARS-CoV-2, T499 and P499.

Therefore, it is unlikely that any form of resistance to the virus, related to the ACE2 gene, exists. However, this analysis merits to be investigated in depth in different ethnic groups for a better assessment of the contribution of genetic variability in host-pathogen interaction.

The similar values of binding energy scores with different ACE2 orthologues suggest that the ability of binding to different ACE2 orthologues is



12

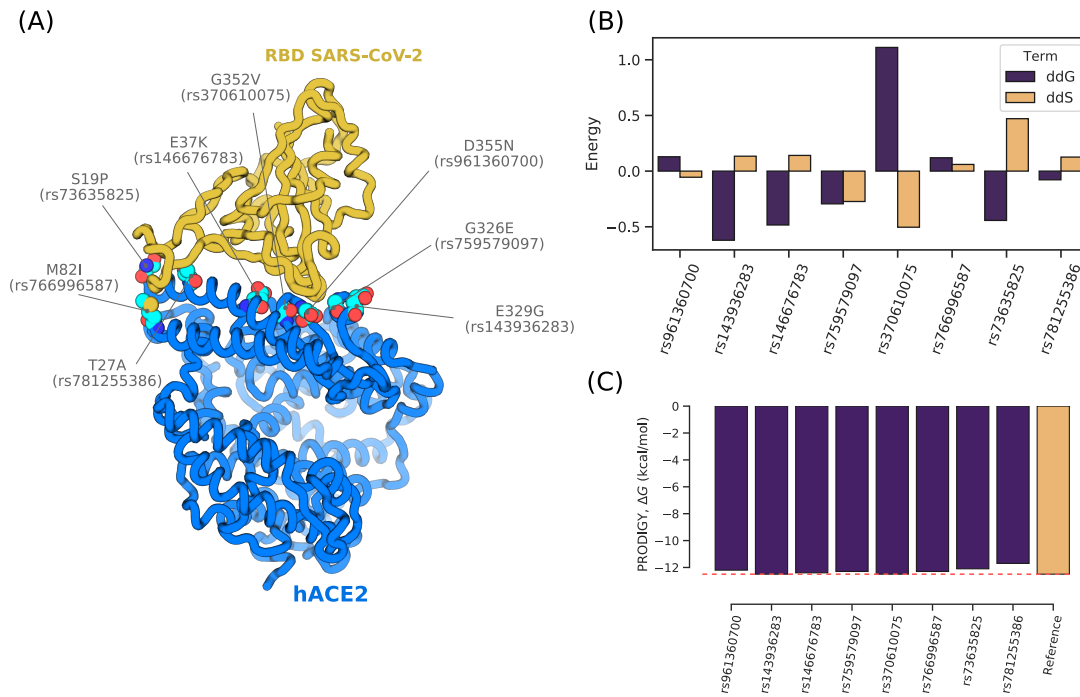


**Figure 4.** Analyzing the interaction of SARS-CoV-2 RBD with different variants of hACE2. (A) Localization of the variants, labeled by the amino acid change and the dbSNP ID, on the interaction surface of hACE2 and RBD from SARS-CoV-2. Estimation of the changing upon mutation for hACE2 variants calculated for enthalpy (ddG) and entropy (ddS) terms of the folding energy calculated with DynaMut (B) and the interaction energy calculated with PRODIGY (D).

preserved in many species either for SARS-CoV-2 or SARS-CoV. Therefore, 233  
the transition to the zoonotic form is trivial if that depends only on ACE2 234  
as the primary route to the infection in both the intermediate and the 235  
final host. However, we know that such a process is very complex since it 236  
requires many protein-protein interactions to acquire the specific capacity 237  
of infecting and replicating in the host cells [18]. Consequently, it makes 238  
sense to assume that many other types of receptors or co-receptors may 239  
be critical to determine the capacity of crossing the species barrier. This 240  
has been already suggested for SARS-CoV [1] and similarly, SARS-CoV-2 241  
may show the same feature. Moreover, our results show that the significant 242  
overlap of glycosylation sites with the protein-protein interface implies a 243  
likely interaction of SARS-CoV-2 progenitors with receptors other than 244  
ACE2. Finally, recent transcriptomic profiling has suggested the possibility 245

of multiple route infections via the interaction of many human receptors 246  
for SARS-CoV-2 [11]. 247

Whole-genome phylogenetic analysis of the different isolates included in 248  
this study is consistent with previous works that place the Wuhan-Hu-1 249  
isolate close to Bat-SL-CoVZC45 and Bat-SL-CoVZXC21 isolates [10, 17] 250  
within the Betacoronavirus genus. The use of RBD sequences, however, 251  
places the virus in a clade that comprises SARS-CoV related homologs 252  
including isolates from Bat and Civet. The clade swapping as seen in 253  
figure 1A, seems also to occur for RaTG13 and Rm1 isolated from bat. This 254  
is expected as the use of different phylogenetic markers may considerably 255  
affect the topology of the tree. However, The significant divergence in 256  
the interfaces segments as a key molecular element contributing to the 257  
determination of the tree topology has driven our work toward studying 258  
their impact on the interaction with hACE2. The binding of the spike 259  
glycoprotein to ACE2 receptor requires a certain level of affinity. In the 260  
case where the RBD evolves from an ancestral form closer to that of Bat-SL- 261  
CoVZC45 and Bat-SL-CoVZXC21, we expected a decrease of the binding 262  
energy scores through the evolution process following incremental changes in 263  
the RBD. In such a scenario, we presume that there are other intermediary 264  
forms of coronavirus that describe such variation of the binding energy 265  
score to reach a level where the pathogen can infect humans with high 266  
affinity toward hACE2. On the other hand, our results show that the 267  
binding energy score and the interface sequence of SARS-CoV-2 RBD are 268  
closer to SARS-CoV related isolates (either from Human or other species). 269  
Therefore a recombination event involving the spike protein that might 270  
have occurred between SARS-CoV and an ancestral form of the current 271  
SARS-CoV-2 virus might be also possible. This will allow for the virus to 272  
acquire a minimum set of residues for the interaction with hACE2. The 273  
recombination in the spike protein gene has been previously suggested 274  
by Wei et al in their phylogenetic analysis [4]. Thereafter, incremental 275  
changes in the binding interface segment will occur in order to reach a 276  
better affinity toward the receptor. One of these changes may involve P499 277  
residue which substitution to threonine seems to drastically destabilize the 278  
interface segment and has a distant effect. Moreover, the decomposition 279  
of the interaction energy showed that 5 out of 6 hotspot amino acids in 280

SARS-CoV-2 have their equivalent in SARS-CoV including N501. Contrary 281  
to what Wan et al [17] have stated, the single mutation N501T does not 282  
seem to enhance the affinity. Rather, the residue Q493 might be responsible 283  
for such higher affinity due to a better satisfaction of the Van der Waals 284  
by the longer polar side chain of asparagine. Indeed, when we made the 285  
same analysis while mutating Q493 to N493, the favorable contribution 286  
decreases from -2.55 kcal/mol to a non significant value of -0.01 kcal/mol, 287  
thus supporting our claim. 288

No major divergence of the interaction interface of SARS-CoV-2 RBD 289  
with hACE2 was noticed from the similarity matrix analysis. This suggests 290  
that the molecular elements required for the binding with the receptor might 291  
also be involved in the interaction with other orthologous forms of ACE2 292  
and that these elements are not optimized specifically for the human form. 293  
Therefore, it is unlikely that the interface of RBD from SARS-CoV-2 is a 294  
result of human intervention via genetic engineering aiming to increase the 295  
affinity toward ACE2. For example, residue E484 contributes unfavorably 296  
to the binding energy with 2.24 kcal/mol due to an electrostatic repulsion 297  
with E75 from hACE2. This residue is an apparent choice for engineering 298  
a protein-protein complex with high affinity by substituting E484 with a 299  
polar residue. It is, however, noteworthy that the lesser homogeneity of the 300  
nodes of SARS-CoV-2 group, in comparison to SARS-CoV, may suggest 301  
a higher tolerance for the mutation of the new virus which would allow 302  
it to cross the species barrier more easily and to efficiently optimize the 303  
interaction in the host. 304

## Declaration of competing interest 305

None of the authors has financial interests or conflicts of interest related to 306  
this research. 307

## Acknowledgement 308

This work was supported by the South African National Research Founda- 309  
tion (NRF) and the Tunisian Ministry of Higher Education and Scientific 310  
Research. The author H. Othman would like to thank Shahine Othman for 311

being understanding about his absence and for not being able to bring him 312  
the marshmallow candy because of the COVID-19 outbreak. 313

## References 314

1. M. Bolles, E. Donaldson, and R. Baric. SARS-CoV and emergent 315  
coronaviruses: viral determinants of interspecies transmission. Curr 316  
Opin Virol, 1(6):624–634, Dec 2011. 317
2. J. F. Chan, S. Yuan, K. H. Kok, K. K. To, H. Chu, J. Yang, F. Xing, 318  
J. Liu, C. C. Yip, R. W. Poon, H. W. Tsoi, S. K. Lo, K. H. Chan, V. K. 319  
Poon, W. M. Chan, J. D. Ip, J. P. Cai, V. C. Cheng, H. Chen, C. K. 320  
Hui, and K. Y. Yuen. A familial cluster of pneumonia associated with 321  
the 2019 novel coronavirus indicating person-to-person transmission: 322  
a study of a family cluster. Lancet, 395(10223):514–523, Feb 2020. 323
3. J. Delgado, L. G. Radusky, D. Cianferoni, and L. Serrano. FoldX 5.0: 324  
working with RNA, small molecules and a new graphical interface. 325  
Bioinformatics, 35(20):4168–4169, Oct 2019. 326
4. W. Ji, W. Wang, X. Zhao, J. Zai, and X. Li. Cross-species transmis- 327  
sion of the newly identified coronavirus 2019-nCoV. J. Med. Virol., 328  
92(4):433–440, Apr 2020. 329
5. K. Katoh, J. Rozewicki, and K. D. Yamada. MAFFT online ser- 330  
vice: multiple sequence alignment, interactive sequence choice and 331  
visualization. Brief. Bioinformatics, 20(4):1160–1166, 07 2019. 332
6. P. J. Kundrotas, Z. Zhu, J. Janin, and I. A. Vakser. Templates are 333  
available to model nearly all complexes of structurally characterized 334  
proteins. Proc. Natl. Acad. Sci. U.S.A., 109(24):9438–9441, Jun 2012. 335
7. M. Kurcinski, T. Oleniecki, M. P. Ciemny, A. Kuriata, A. Kolinski, 336  
and S. Kmiecik. CABS-flex standalone: a simulation environment for 337  
fast modeling of protein flexibility. Bioinformatics, 35(4):694–695, 338  
02 2019. 339

8. J. Lan, J. Ge, J. Yu, S. Shan, H. Zhou, S. Fan, Q. Zhang, X. Shi, 340  
Q. Wang, L. Zhang, and X. Wang. Crystal structure of the 2019-ncov 341  
spike receptor-binding domain bound with the ace2 receptor. bioRxiv, 342  
2020. 343
9. I. Letunic and P. Bork. Interactive Tree Of Life (iTOL) v4: recent 344  
updates and new developments. Nucleic Acids Res., 47(W1):W256– 345  
W259, Jul 2019. 346
10. D. Paraskevis, E. G. Kostaki, G. Magiorkinis, G. Panayiotakopoulos, 347  
G. Sourvinos, and S. Tsiodras. Full-genome evolutionary analysis 348  
of the novel corona virus (2019-nCoV) rejects the hypothesis of 349  
emergence as a result of a recent recombination event. Infect. Genet. 350  
Evol., 79:104212, Apr 2020. 351
11. F. Qi, S. Qian, S. Zhang, and Z. Zhang. Single cell RNA sequencing 352  
of 13 human tissues identify cell types and receptors of human 353  
coronaviruses. Biochem. Biophys. Res. Commun., Mar 2020. 354
12. P. Rice, I. Longden, and A. Bleasby. EMBOSS: the European Molec- 355  
ular Biology Open Software Suite. Trends Genet., 16(6):276–277, 356  
Jun 2000. 357
13. C. H. Rodrigues, D. E. Pires, and D. B. Ascher. DynaMut: predicting 358  
the impact of mutations on protein conformation, flexibility and 359  
stability. Nucleic Acids Res., 46(W1):W350–W355, 07 2018. 360
14. A. Sali and T. L. Blundell. Comparative protein modelling by sat- 361  
isfaction of spatial restraints. J. Mol. Biol., 234(3):779–815, Dec 362  
1993. 363
15. M. Y. Shen and A. Sali. Statistical potential for assessment and 364  
prediction of protein structures. Protein Sci., 15(11):2507–2524, Nov 365  
2006. 366
16. K. Tamura, G. Stecher, D. Peterson, A. Filipski, and S. Kumar. 367  
MEGA6: Molecular Evolutionary Genetics Analysis version 6.0. Mol. 368  
Biol. Evol., 30(12):2725–2729, Dec 2013. 369

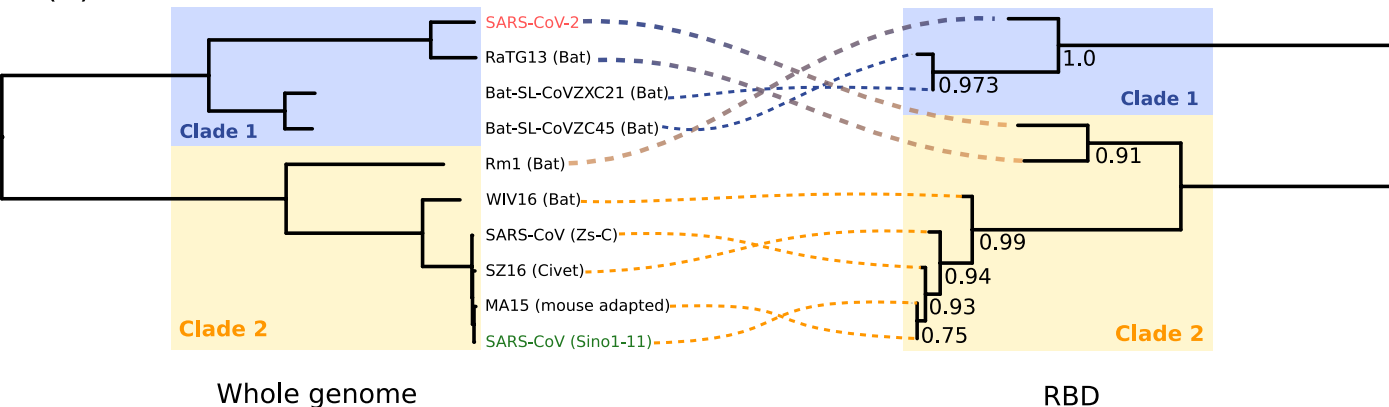
17. Y. Wan, J. Shang, R. Graham, R. S. Baric, and F. Li. Receptor recognition by novel coronavirus from Wuhan: An analysis based on decade-long structural studies of SARS. J. Virol., Jan 2020.
18. C. J. Warren and S. L. Sawyer. How host genetics dictates successful viral zoonosis. PLoS Biol., 17(4):e3000217, 04 2019.
19. G. Weng, E. Wang, Z. Wang, H. Liu, F. Zhu, D. Li, and T. Hou. HawkDock: a web server to predict and analyze the protein-protein complex based on computational docking and MM/GBSA. Nucleic Acids Res., 47(W1):W322–W330, Jul 2019.
20. S. Whelan and N. Goldman. A General Empirical Model of Protein Evolution Derived from Multiple Protein Families Using a Maximum-Likelihood Approach. Molecular Biology and Evolution, 18(5):691–699, 05 2001.
21. D. Wrapp, N. Wang, K. S. Corbett, J. A. Goldsmith, C. L. Hsieh, O. Abiona, B. S. Graham, and J. S. McLellan. Cryo-EM structure of the 2019-nCoV spike in the prefusion conformation. Science, Feb 2020.
22. L. C. Xue, J. P. Rodrigues, P. L. Kastritis, A. M. Bonvin, and A. Vangone. PRODIGY: a web server for predicting the binding affinity of protein-protein complexes. Bioinformatics, 32(23):3676–3678, 12 2016.
23. R. Yan, Y. Zhang, Y. Guo, L. Xia, and Q. Zhou. Structural basis for the recognition of the 2019-ncov by human ace2. bioRxiv, 2020.

**Table 1.** Population frequencies of hACE2 missense variants located on the interaction surface with SARS-CoV-2 RBD ( $\times 10^{-5}$ )

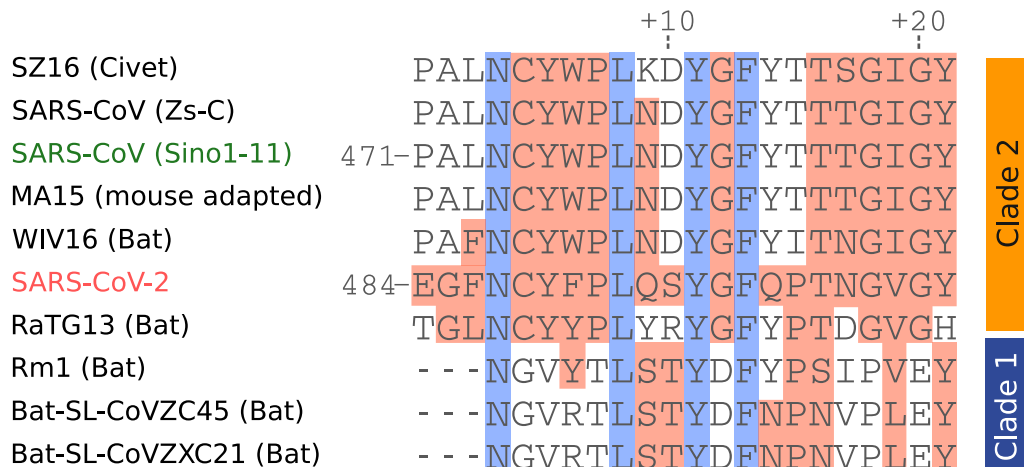
rs ID	European (non-Finnish)	African	Latino	Ashkenazi Jewish	East Asian	South Asian	Finnish	Other	Global
rs961360700	2.59	0	0	0	0	0	0	0	1.17
rs143936283	6.51	0	0	0	0	0	0	19.05	3.443
rs146676783	0	0.105	0	0	0	0	32.22	0	3.897
rs759579097	0	0.1056	0	0	0	0	0	0	0.9842
rs370610075	1.274	0	0	0	0	0	0	0	0.5752
rs766996587	0	26.23	0	0	0	0	0	0	2.442
rs73635825	0	332.3	0	0	0	0	0	18.82	31.29
rs781255386	0	0	7.303	0	0	0	0	0	1.091



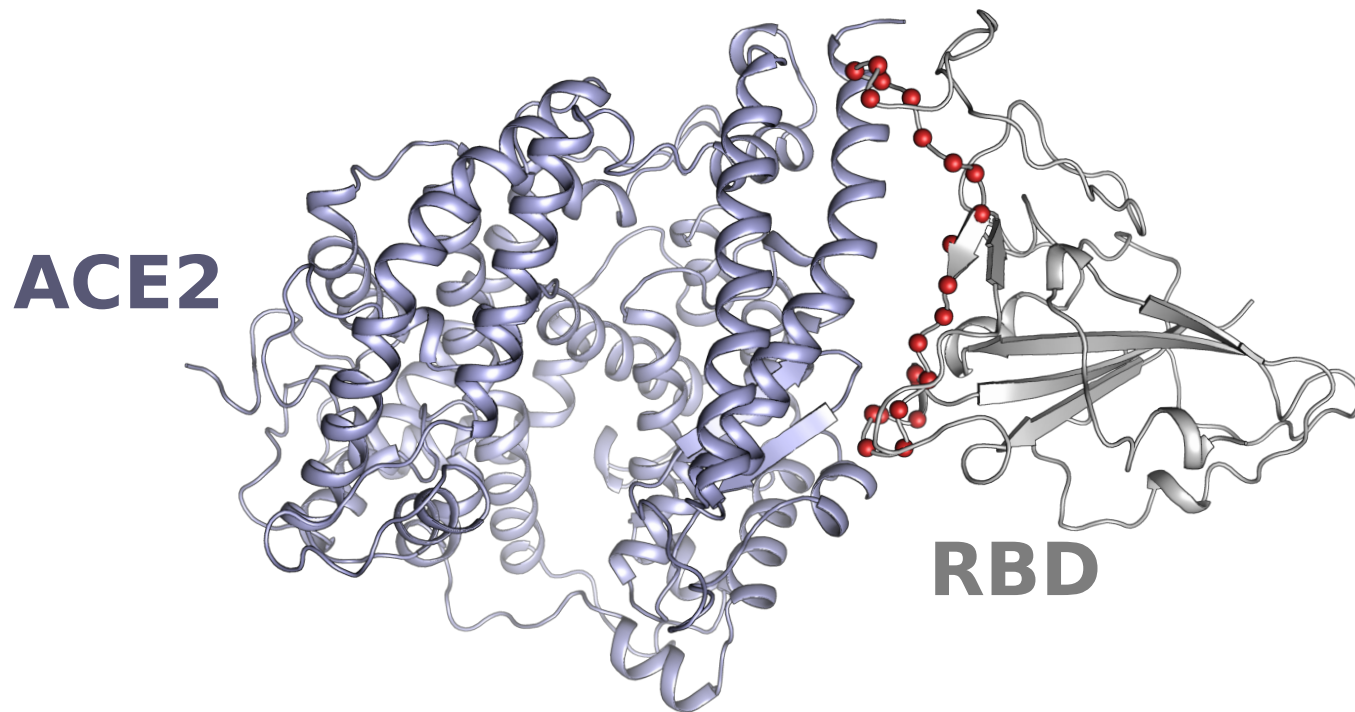
(A)



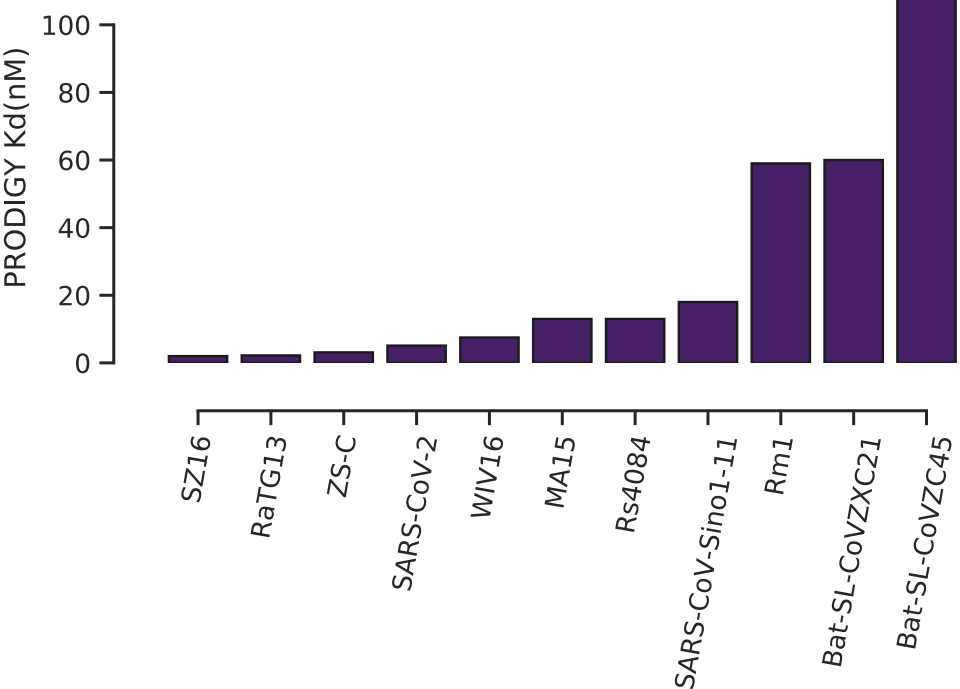
(B)



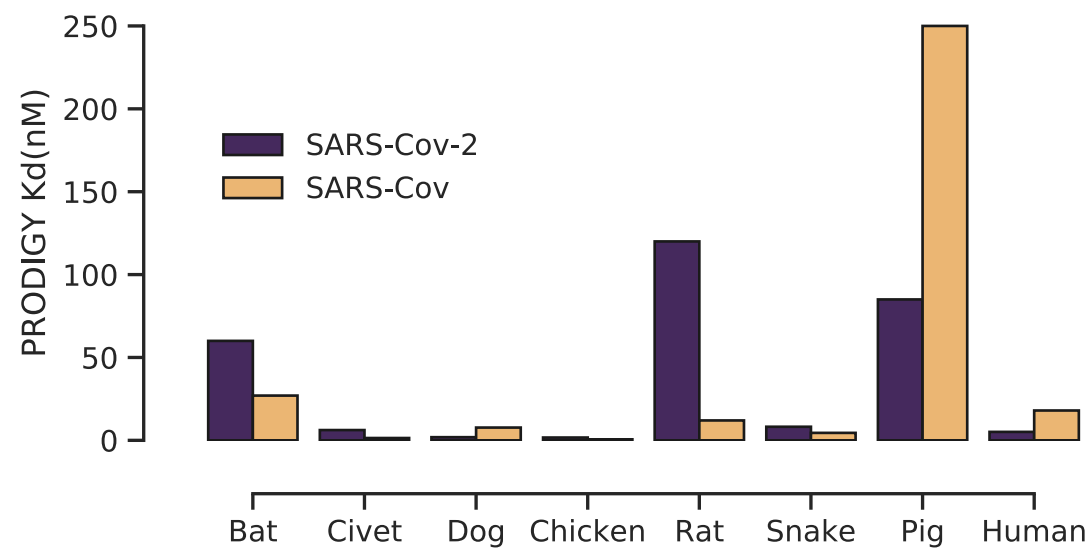
(A)



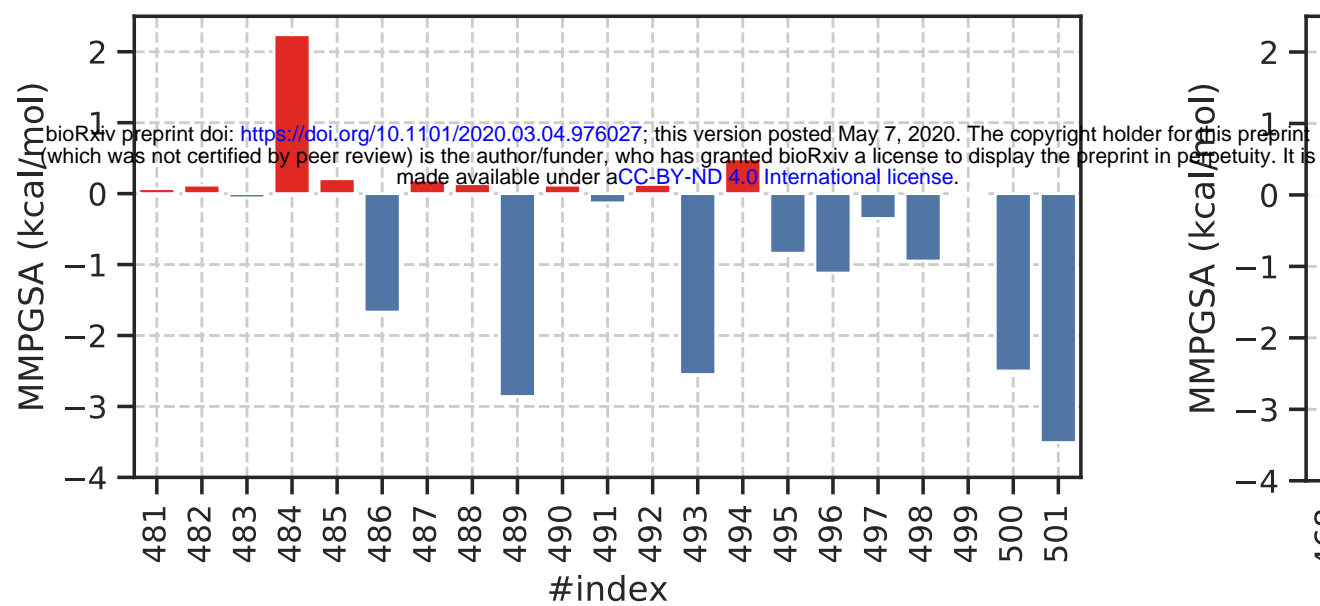
(B)



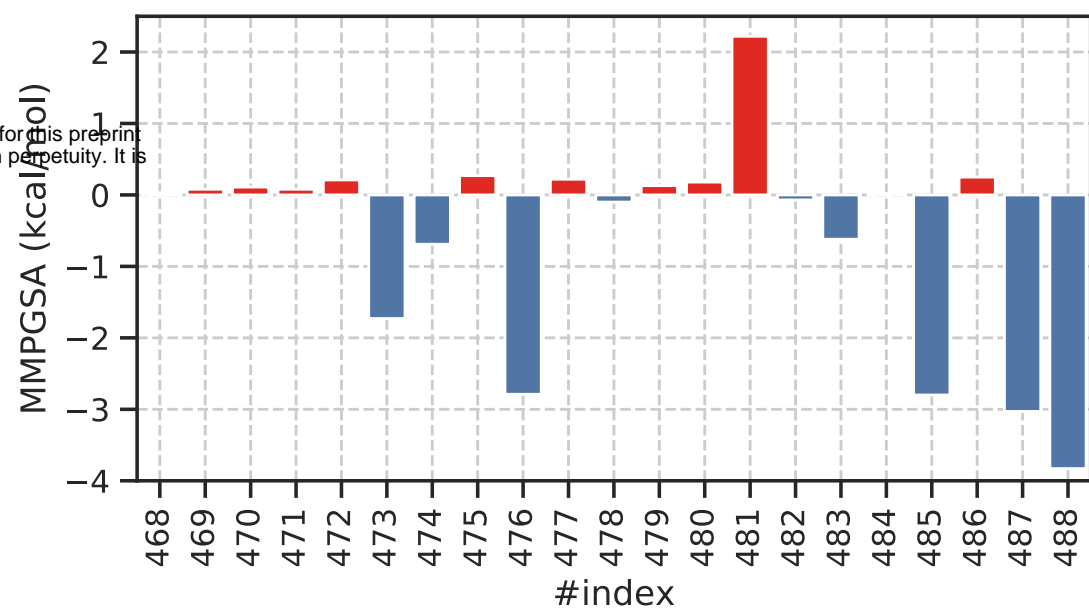
(C)



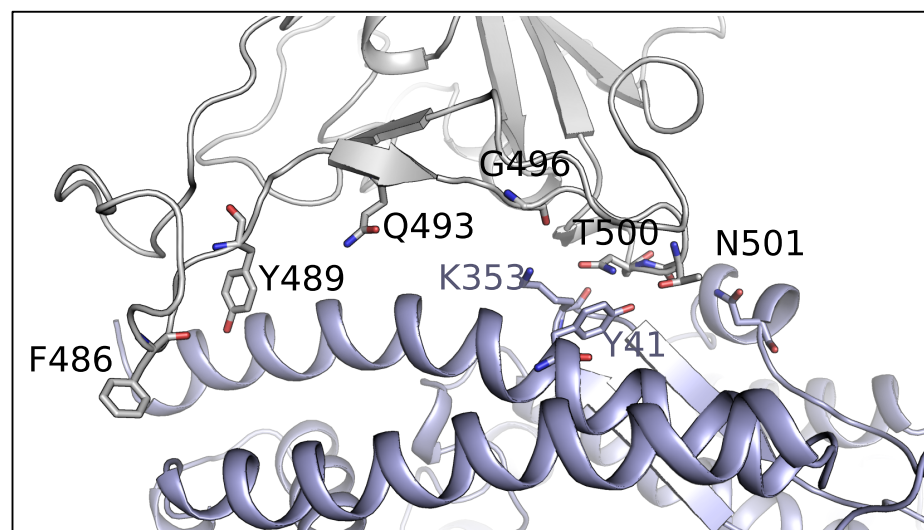
(A)



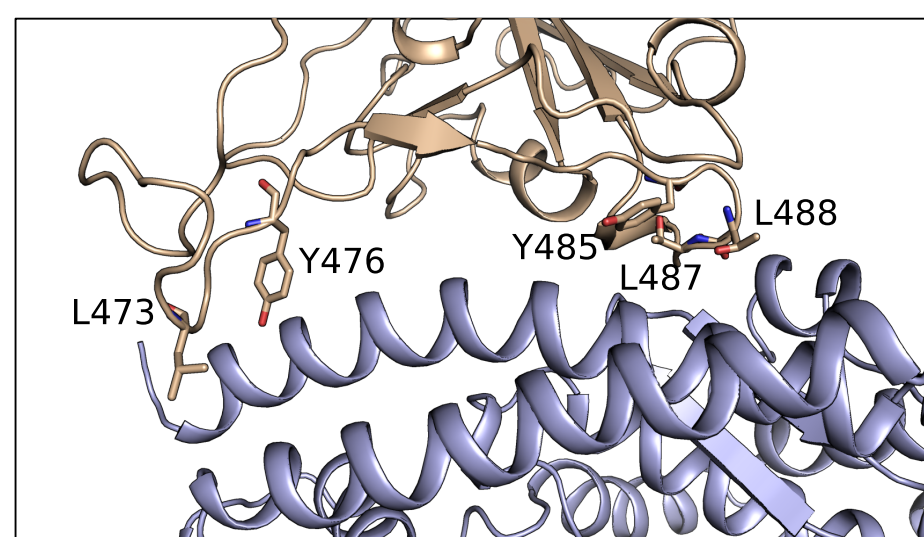
(B)



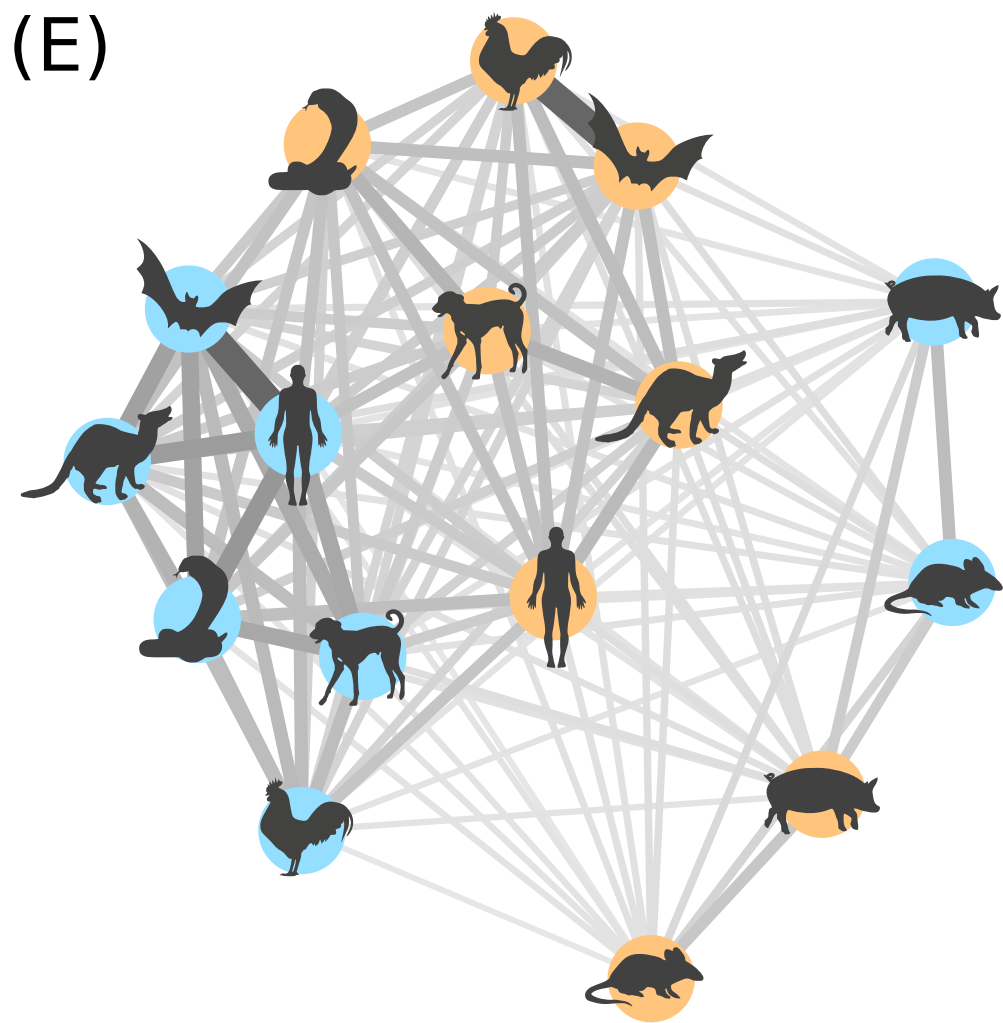
(C)



(D)

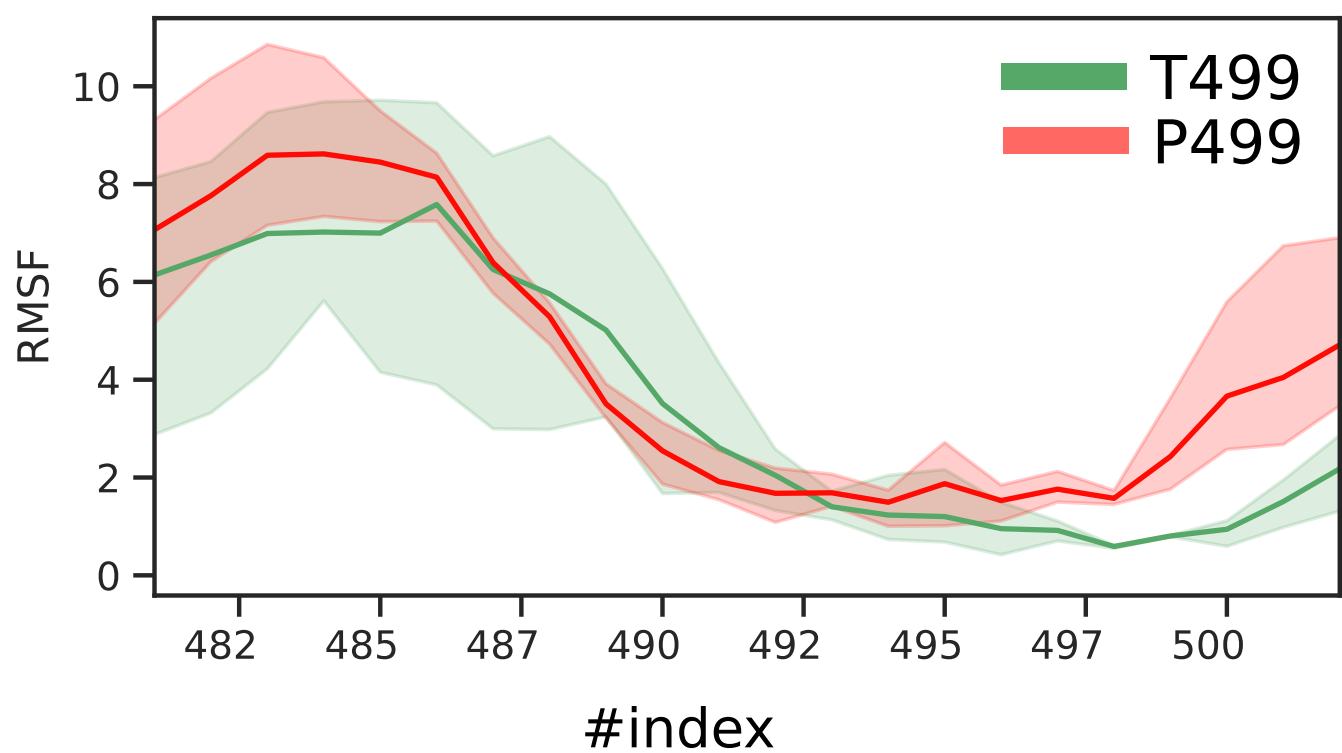


(E)

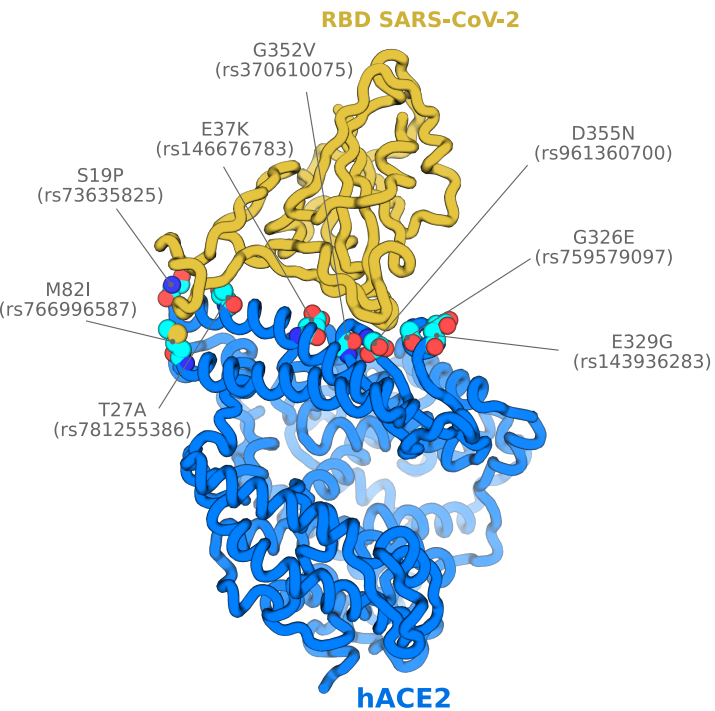


○ SARS-CoV-2      ○ SARS-CoV

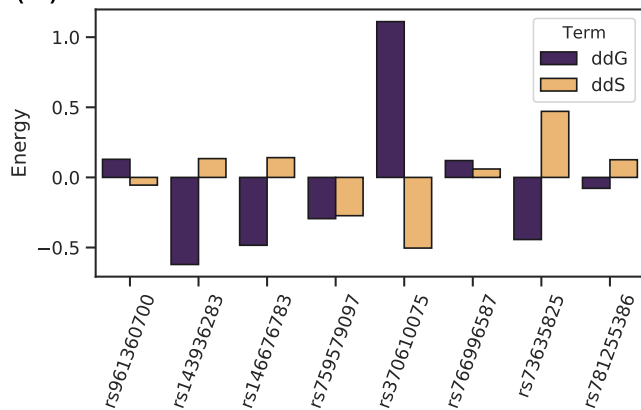
(F)



(A)



(B)



(D)

